Science of the Total Environment 643 (2018) 1610–1622

Contents lists available at ScienceDirect

Science of the Total Environment

journal homepage: www.elsevier.com/locate/scitotenv

Integrated assessment of the climate and landuse change impact on hydrology and water quality in the Songkhram River Basin, Thailand

Sangam Shrestha [a,*], Binod Bhatta [a], Manish Shrestha [a,b], Pallav K. Shrestha [a,c]

[a] Water Engineering and Management, School of Engineering and Technology, Asian Institute of Technology, P.O. Box 4, Klong Luang, Pathum Thani 12120, Thailand
[b] Stockholm Environment Institute, Chulalongkorn Soi 64, Phyathai Road, Pathumwan, Bangkok, 1033 Thailand
[c] Computational Hydrosystems, Helmholtz Centre for Environmental Research - UFZ, Permoserstraße 15, Leipzig 04315, Germany

HIGHLIGHTS

- Climate and landuse change impact on hydrology and water quality were assessed.
- SWAT and DynaCLUE models were used to simulate hydrology and landuse change.
- Greater impacts were estimated by climate change compared to landuse change.
- Combined climate and landuse change decreased streamflow and nitrate loading.

GRAPHICAL ABSTRACT

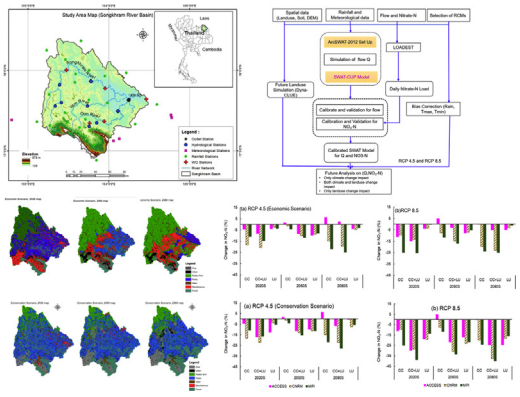

ARTICLE INFO

Article history:
Received 11 March 2018
Received in revised form 25 June 2018
Accepted 25 June 2018
Available online 4 July 2018

Editor: D. Barcelo

Keywords:
Climate change
Landuse change
Streamflow
Water quality
SWAT
Dyna-CLUE

ABSTRACT

The livelihoods of people in the Songkhram River Basin (SRB) rely heavily on river water, especially those involved in the fisheries. Extensive landuse changes in SRB have raised concerns regarding its impacts in water quality in addition to the looming climate change effects. More importantly there is lack of detailed studies on landuse and climate change impact on river water quality for the sustainable water management. Therefore, this study aimed at quantifying the individual and integrated impact of climate and landuse change in streamflows and nitrate nitrogen loadings in the Songkhram River. Future streamflow was simulated using Soil and Water Assessment Tool (SWAT) whereas future climate projections were derived from three Regional Climate Models (RCMs) under two Representative Concentration Pathways (RCPs). A dynamic, spatially explicit, land use change model (Dyna-CLUE) was used to generate two future land use change scenarios namely economic and conservation scenarios. The results show that in future climate change is to be responsible for a 19.5 and 24% decrease in streamflow and 11.25 and 15.25% decrease in nitrate nitrogen loading as projected under RCP 4.5 and 8.5 scenarios, respectively. Whereas landuse change is found to be responsible for a 5.30 and 6.35% increase in streamflow and an 11 and 11.60% decrease in nitrate nitrogen loading under economic and conservation scenarios, respectively in future. Thus, in conjunction, these two agents are seen to play against each other, creating a net effect of decreased future streamflow (16% on average); whereas, in the case of nitrate nitrogen loading, the two work in tandem, leading to an amplified reduction (24.50% on average). Although

* Corresponding author.
E-mail address: sangam@ait.ac.th (S. Shrestha).

https://doi.org/10.1016/j.scitotenv.2018.06.306
0048-9697/© 2018 Elsevier B.V. All rights reserved.

landuse change is found to be the less afflicting agent, its role should not be overlooked—it may very well further exacerbate the situation if there is a greater unfavourable climatic variation than projected.

© 2018 Elsevier B.V. All rights reserved.

1. Introduction

Rapid population growth, unplanned urbanization and landuse and land cover changes have been recognized as major challenges for water resources management (Hunter, 2003). Land use and land cover change can alter the basin hydrology by affecting evaporation, soil infiltration capacity, and surface and subsurface regimes and ultimately affecting water quantity and water quality (Cuo et al., 2013). In recent decades, changes in land use patterns and farming practices caused by demographics, economics, or cultural alternation, have significantly affected water quality (Berka et al., 2001). As a consequence, water is becoming polluted by nutrients, increasing the eutrophication hazards. Eutrophication is a continuous problem for water engineers and managers (Daniel et al., 1998). In addition to the current water management challenges, climate change is an additional challenge for sustainable water resources management. Climate change is considered as a critical factor in the prediction and evaluation of the future water resources (Kim et al., 2013). The climate change result changes in seasonal and annual streamflow which in turn affect hydrological characteristics of watershed (Murray-Hudson et al., 2006; Novotny and Stefan, 2007; Heathwaite, 2010). Climate change also brings about alterations in the sediment flux and the river morphology, which in turn will affect the river ecosystems. The risks associated with extreme events of climate change are found to be high with an extra 1 °C increase in warming. It is projected that the water availability is expected to change in many tropical and sub-tropical zones in future (IPCC, 2014).

Various studies show that landuse and land cover change and climate change are the two essential factors affecting water availability and water quality (Li et al., 2012; El-Khoury et al., 2015; Mehdi et al., 2015; Pulido-Velazquez et al., 2015; Shrestha et al., 2016). All of these studies have followed the modelling approaches to evaluate the impacts for water resources planning and evaluation. Climate and land use changes may interact and thus have combined impacts on water availability and water quality and the consequences are uncertain. Tu in 2009 (Tu, 2009) estimated the combined impact of climate and land use changes on streamflow and water quality in eastern Massachusetts, USA. The study found out that climate change and land development have more impact on changing the seasonal distributions of the streamflow and nitrogen load than on altering average annual amounts of the streamflow and nitrogen load. Kim et al., 2013 examined the impacts of changes in climate and land use/land cover under IPCC RCP scenarios on streamflow in the Hoeya River Basin, Korea. It was found that the effects of LULC change were smaller than those caused by climate change. Whereas the effect of LULC change on streamflow was very significant. El-Khoury et al., 2015 investigated the combined impacts of future climate and landuse changes on discharge, nitrogen and phosphorus loads for a Canadian river basin. They found out that changes in streamflow will mainly be driven by climate change whereas changes in nitrogen species will mainly be driven by land use changes. The contributions of both factors on organic and mineral phosphorus are roughly equal. Pulido-Velazquez et al., 2015 assessed the impact of climate and land use changes on groundwater quantity and quality in the Mancha Oriental system in Spain. The results show the response of groundwater quantity and quality (nitrate pollution) to climate and land use changes, with decreasing groundwater recharge and an increase in nitrate concentrations. Mehdi et al., 2015 evaluated the impacts of climate change and crop land use change on streamflow, nitrates and phosphorus in Bavaria, Germany. It was estimated that climate change impacts deteriorate surface water quality in future and the impacts were amplified when landuse change scenarios were considered with climate change. The total phosphorus and nitrate nitrogen were estimated to increase in the combined scenarios for each month. Trang et al., 2017 evaluated the impacts of climate and landuse change on the hydrology and nutrient yield in a 3S River Basin, transboundary river basin in Southeast Asia. The discharge and nutrient loadings was projected to increase in wet season whereas it was projected to decrease in dry season.

All the existing studies described above have some limitations such as use of future climate data of old emission scenarios (Special Report on Emission Scenarios, SRES); use of future climate data from single climate model or use of future land use predicted by simple regression models. These limitations can bring uncertainties in impact assessment on hydrology and water quality. Therefore, this study used future climate data of new emission scenarios (Representative Concentration Pathways, RCP) from multiple climate models. Similarly, future land use change was forecasted using dynamic landuse and land cover simulation model (Dyna-CLUE) to address the uncertainties. The overall objective of this study is to quantify the individual and integrated impacts of climate and landuse change on streamflow and water quality (nitrate nitrogen) of the Songkhram River Basin. The sub-objectives are: (i) investigating future climate change constructed using linear scaling bias correction method; (ii) analysis of landuse change pattern of the past, present and future by Dyna-CLUE model; and (iii) stream flow and nitrate nitrogen loading estimation in view of (a) only climate change impact on streamflow and nitrate nitrogen loading, (b) only landuse change impact on streamflow and nitrate nitrogen loading, and (c) combined impact of both on streamflow and nitrate nitrogen loading.

2. Study area and data collection

2.1. Study area

The Songkhram River Basin (SRB) is the second largest catchment in northeast Thailand (Fig. 1). It drains a catchment of 12,880 km^2 into the Mekong River. The elevation of the basin varies from 135 to 675 m from the mean sea level with a gentle slope of 1:30,000 (Shrestha and Muangthong, 2014). The Yam and Oon Rivers are the major tributaries of the Songkhram River.

The SRB has a tropical semi-arid climate with three distinct seasons, namely summer (Jan–Apr), rainy (May–Oct), and winter (Nov–Dec) with more than 90% of annual rainfall in the rainy season. There is distinct spatial variation in rainfall within the basin. On average, the annual rainfall in the southern part is 1200 mm and 2100 mm in the northern. High temperatures are common from March to the middle of May, during which it can exceed 40 °C. The minimum temperature seldom falls below 10 °C, even during winter. Understandably, the SRB has a high and variable annual evaporation rate ranging from 1550 to 2054 mm/-year (Blake and Pitakthepsombut, 2006). The SRB has a high seasonal flow with an average annual discharge of about 350 m^3/s. The peak discharge events are observed during the months of August and September.

The downstream part of the SRB (also known as the Lower Songkhram River Basin), is a floodplain covering an area of around 3000 km^2. The Thai government considers it a wetland of international importance (Blake and Pitakthepsombut, 2006). A number of different wetland habitats such as swamps, pools, main river channels, ox-bow

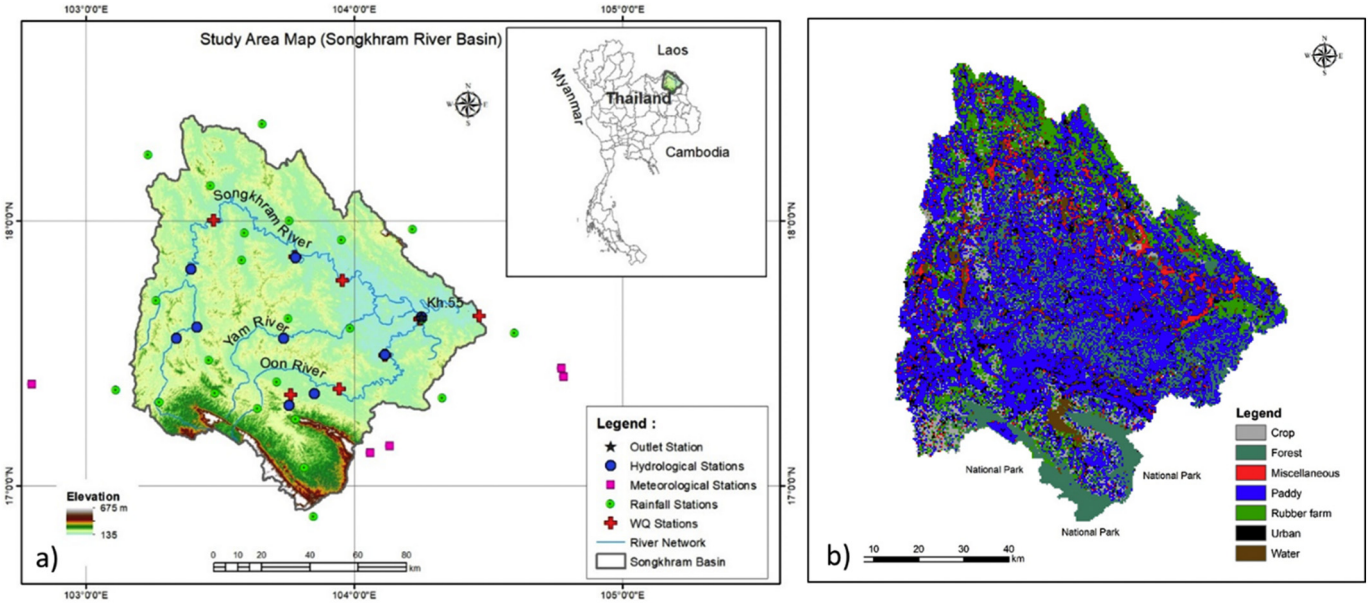

Fig. 1. Location (a) and landuse map (2009) (b) of the Songkhram River Basin (SRB).

lakes, grasslands, etc. are found in the floodplains of the Lower Songkhram River Basin.

Agricultural land is the major donor of solutes pertaining to river water quality, including nitrates. With better annual rainfall, the northern part of the SRB is suitable for cultivation especially paddy. In the SRB, landuse is dominated by agricultural land—paddy fields represent more than 48% of total landuse.

2.2. Data collection

The datasets used in this study comprise the physical characteristics of the catchment (elevation, soil, and landuse), time series observations (climate, hydrology, and water quality), and future climate projections from climate models (Table 1).

2.2.1. Historical landuse change and future landuse and climate change scenarios

In this study, the historical landuse maps of 2009 and 2014 were obtained from LDD, Thailand and changes were analysed. The percentage area under each landuse in 2009 and 2014 is shown in Table 2. The urban (built- up area) increased from 3.7% in 2009 to 4.3% in 2014. Similarly, the planted trees landuse type has also increased from 14.4% to 18% by 2014 with an increasing rate of 5.13% per year. However, decrease in crop, paddy and forest areas at the rate of 2.91%, 1.64% and 2.16% were observed within those five years.

The future landuse maps in SRB were simulated by considering following two potential landuse change scenarios, based on the Thai government's restrictions for landuse change.

2.2.1.1. Economic scenario. In this scenario more than half of the basin area will be covered by rubber plantation if the rate of landuse change remains the same as in the past as found in Table 2.

2.2.1.2. Conservation scenario. In this scenario, no landuse changes are allowed on the proposed Ramsar site and national park. Under this scenario (an increase in forest area to 25% of land by 2100), natural forest will gradually start to expand from the area of the national park, covering 22% by the middle of the century. This scenario restricts rapid expansion of the built-up area which will cover only 6% of the total. The

Table 1
Data and corresponding sources.

SN	Data	Source/Developer	Spatial/Temporal resolution	Number/Time period
Physical characteristics of the catchment				
1	Elevation	ASTER GDEM version 2	30 m/—	–
2	Soil	FAO/UNESCO—the digital soil map of the world	1:5,000,000/—	–
3	Landuse	Land Development Department (LDD) Thailand	1 km/—	2 maps—2009, 2014
Time series observations				
1	Meteorology	Thai Meteorological Department (TMD)	Point/Daily	30 (rain stations), 6 (climatic stations)/1975–2014
2	Hydrology	Royal Irrigation Department (RID) Thailand	Point/Daily	1 station/1990–2014
3	Water Quality	Pollution Control Department (PCD) Thailand	Point/3 to 4 times a year	9 stations/2005–2015

SN	Data	Source/Developer	Spatial/Temporal resolution	Parent GCM	Number/Time period
RCMs data for future climate projections					
1	ACCESS-CSIRO-CCAM	Collaboration for Australia Weather and Climate Research, Australian Government	0.5^0/Daily	ACCESS1.0	RCP 4.5 and 8.5/1975–2099
2	CNRM-CM5-CSIRO-CCAM	National Centre for Meteorological Research	0.5^0/Daily	CNRM-CM5	RCP 4.5 and 8.5/1975–2099
3	MPI-ESM-LR-CSIRO-CCAM	European Network for Earth System Modelling	0.5^0/Daily	MPI-ESM-LR	RCP 4.5 and 8.5/1975–2099

Table 2
Land use area in SRB for the periods of 2009 and 2014.

Code	Aggregated class	Thai landuse classification	2009	2014	% Change/year
0	Crop	Field crop, Horticulture, Integrated farm/Diversified farm, Orchard/Horticulture, Paddy field crop	5.9%	4.8%	−2.9
1	Urban (Built-up area)	Village, Village, Transportation, Communication and Utility, Industrial land, City, Town, Commercial, Village/Orchard, Other built-up land, Pasture and farm house, Institutional land	3.7%	4.3%	3.4
2	Planted trees	Perennial, Orchard, Perennial/Orchard, Forest Plantation, Field crop/Perennial, Field crop/Orchard	14.4%	18.0%	5.1
3	Paddy	Paddy field	48.3%	45.1%	−1.6
4	Water Body	Reservoir (Built-up), Marsh and Swamp, Natural water body, Natural water body, Aquaculture land	4.9%	6.0%	4.8
5	Miscellaneous land	Other miscellaneous land, Mine, pit, Rangeland	5.8%	6.8%	5.5
6	Forest	Evergreen forest, Deciduous forest	17.0%	14.9%	−2.2

basin is assumed to experience a decrease in rubber farms and paddy fields so as to compensate for the expanding forest.

The future climate data of three Regional Climate Models (RCMs) were used to construct the future climate of the region in near future (2010–2039), mid-future (2040–2069) and far future (2070–2099), including high (RCP 8.5) and medium (RCP 4.5) emission scenarios. Firstly, climate in the form of temperature and precipitation was extracted from (ACCESS-CSIRO-CCAM, CNRMCM5-CSIRO-CCAM, and MPI-ESM-LR-CSIRO-CCAM) RCMs (Table 1) and the future climate data was then corrected by the linear scaling method of bias correction using the baseline climate (1975–2009). The Representative Concentration Pathways (RCPs) are four greenhouse gas concentration trajectories (scenarios) adopted by the IPCC for its Fifth Assessment Report (AR5) in 2014. The pathways describe four possible future climates, depending on how much greenhouse gases are emitted in the years to come. The four RCPs: RCP2.6, RCP4.5, RCP6.0, and RCP8.5, are named after a possible range of radiative forcing values in the year 2100 relative to pre-industrial values (+2.6, +4.5, +6.0, and +8.5 W/m^2, respectively). RCP 2.6 assumes that global annual GHG emissions (measured in CO_2-equivalents) peak from 2010 to 2020, declining substantially thereafter. Emissions in RCP 4.5 peak around 2040, and then decline. In RCP 6.0, emissions peak around 2080, and then decline. In RCP 8.5, emissions continue to rise throughout the twenty-first century (Van Vuuren et al., 2011).

3. Research methodology

The potential impacts of climate and landuse change in the SRB during the twenty-first century were analysed for three time windows viz. 2020s (2010–2039), 2050s (2040–2069), and 2080s (2070–2099) for three major scenarios, namely *only climate change*, *only landuse change,* and *combined climate and landuse change*. Fig. 2 illustrates the methodology framework adopted for this study.

3.1. Bias correction of climate data

RCMs help to achieve climate variables at finer resolutions for a region of interest. However, out of hundreds of RCM output grids, only 12 intersect with the boundary of the SRB. It is highly unlikely that the

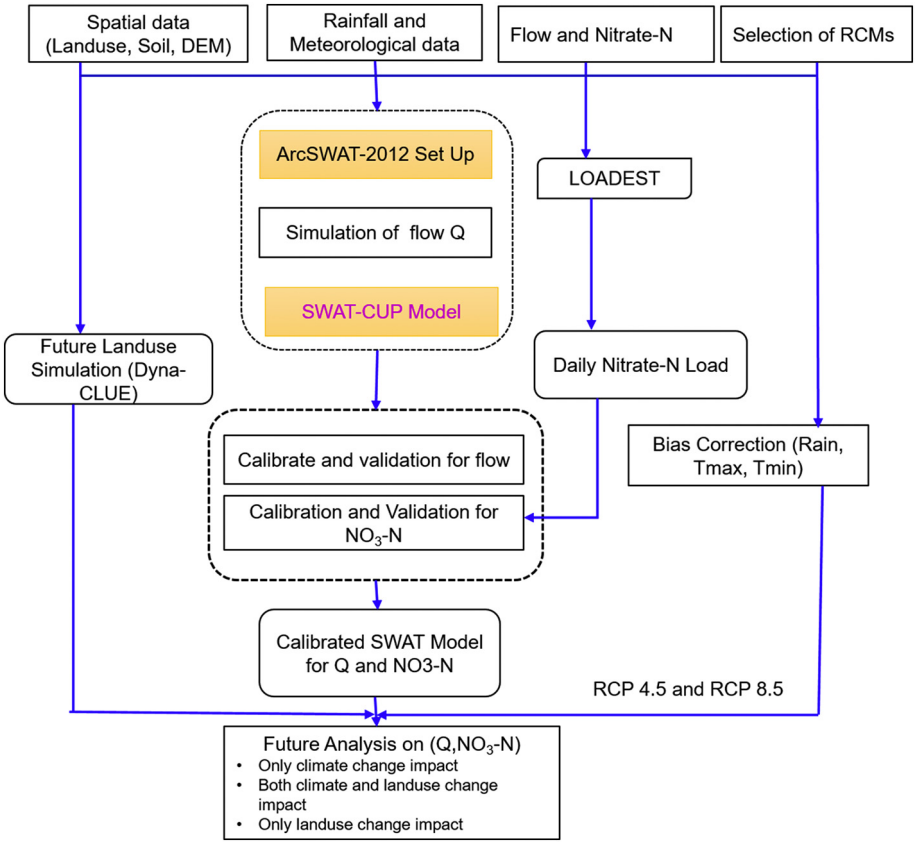
Spatial data (Landuse, Soil, DEM)
Rainfall and Meteorological data
Flow and Nitrate-N
Selection of RCMs
ArcSWAT-2012 Set Up
Simulation of flow Q
SWAT-CUP Model
LOADEST
Future Landuse Simulation (Dyna-CLUE)
Daily Nitrate-N Load
Calibrate and validation for flow
Calibration and Validation for NO3-N
Bias Correction (Rain, Tmax, Tmin)
Calibrated SWAT Model for Q and NO3-N
RCP 4.5 and RCP 8.5
Future Analysis on (Q,NO3-N)
Only climate change impact
Both climate and landuse change impact
Only landuse change impact

Fig. 2. Methodology framework used in this study.

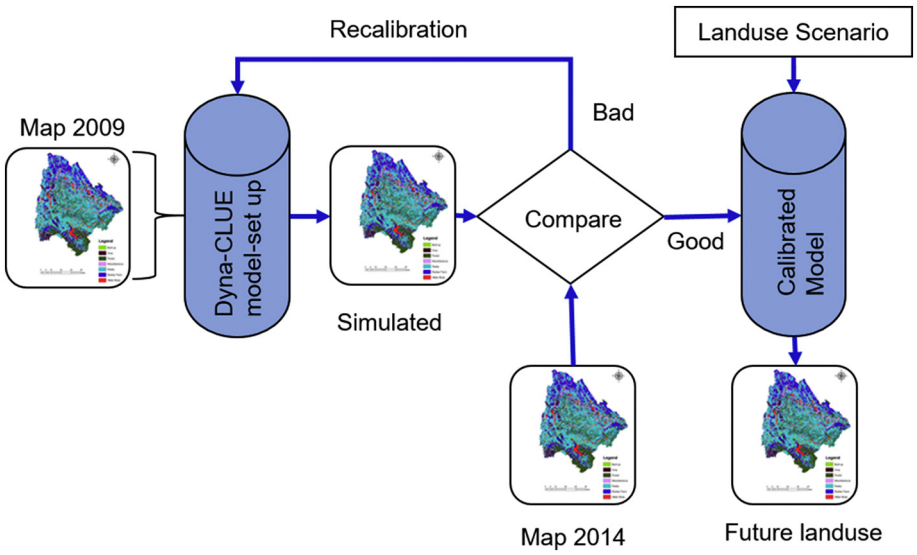

Fig. 3. Framework for Dyna-CLUE modelling in this study.

grids for the SRB sufficiently possess the spatial-temporal variations observed over the basin. Moreover, RCM products generally possess some bias due to a lack of climate model fine tuning for sub-regions or calibration priority for other sub-regions of the RCM domain. To check this, the grid values are compared and corrected for improvement (if any bias is present) using the measurement data. The correction parameters so calculated are applied to the future projection of the RCMs. This process is known as bias correction (Li et al., 2014).

Correction is made for bias present in precipitation and maximum and minimum temperature. The existing bias was corrected using linear scaling (LS) method. LS is the simplest method of bias correction (Ines and Hansen, 2006; Teutschbein and Seibert, 2012) and performs as good as more complex methods for coarse temporal scale analysis (Shrestha et al., 2017) in this case. The following equations were used for the linear scaling technique (Shrestha et al., 2016).

Temperature Correction:

$$T^{*}_{his}(d) = T_{his}(d) + [\mu_m(T_{obs}(d) - \mu_m T_{his}(d))] \quad (1)$$

$$T^{*}_{sim}(d) = T_{sim}(d) + [\mu_m(T_{obs}(d)) - \mu_m(T_{his}(d))] \quad (2)$$

Precipitation Correction:

$$P^{*}_{his} = P_{his}(d) X \left[\frac{\mu_m(P_{obs}(d))}{\mu_m(P_{his}(d))}\right] \quad (3)$$

$$P^{*}_{sim}(d) = P_{sim}(d) X \left[\frac{\mu_m(P_{obs}(d)}{\mu_m(P_{his}(d)}\right] \quad (4)$$

Where, P = precipitation, T = temperature, d = daily, μ_m = long term monthly mean, * = bias corrected, his = Raw RCM historical data, obs = observed/measured data, sim = Raw RCM future data.

3.2. Landuse change modelling

The Dyna-CLUE model was used to simulate future landuse maps. Dyna-CLUE is a non-commercial, widely accepted landuse change simulation model applicable to a wide range of conditions for developing future landuse scenarios based on management policies (Verburg and Overmars, 2009; Zhang et al., 2016). Dyna-CLUE has two modules, namely the *non-spatial (demand) module* and the *spatial allocation module* (Park et al., 2011). The demand module determines the demand of various landuse through past landuse trends or scenario-based landuse,

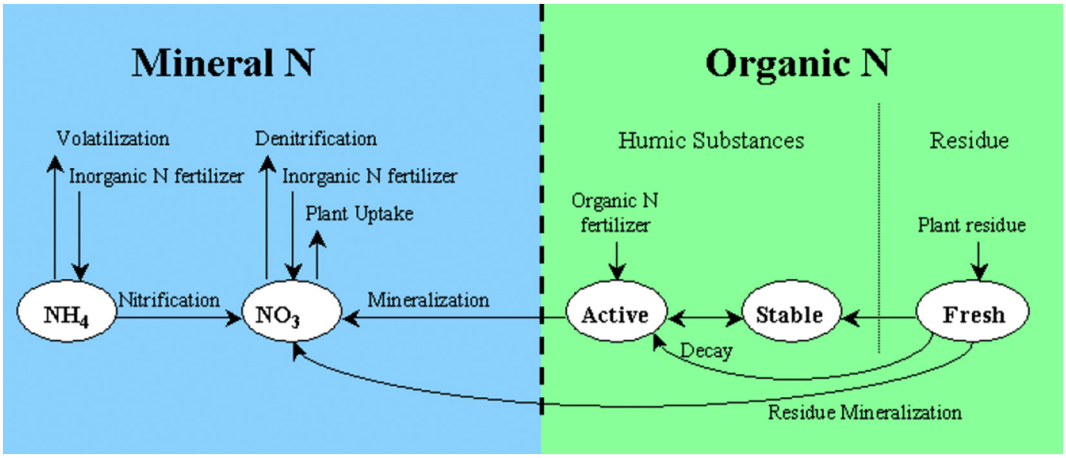

Fig. 4. SWAT soil nitrogen pools and processes that move nitrogen in and out of pools (Neitsch et al., 2011).

Table 3
Sensitivity analysis of SWAT model parameters for streamflow and nitrate with fitted values.

Parameters	Description of the parameter	Range of the parameters	Final value	Sensitivity rank
Hydrology				
CN2.mgt (r)	SCS runoff curve number	[−0.2,0.15]	0.13	1
GW_DELAY.gw (v)	Delay time for aquifer recharge	[30,244.27]	32.50	2
CH_K2.rte (v)	Effective hydraulic conductivity	[0,316.09]	227.06	3
RCHRG_DP.gw (v)	Deep aquifer percolation fraction	[0,0.5]	0.21	4
GW_REVAP.gw (v)	Groundwater "revap" coefficient	[0.02,0.12]	0.03	5
Nitrate				
LAT_ORGN.gw (v)	Organic N in the baseflow (mg/l)	[0,100.91]	2.091	1
BC1.swq (v)	Rate constant for biological oxidation of NH_4 to NO_2 in the reach at 20 °C	[0.1,0.69]	0.630	2
BC2.swq (v)	Rate constant for biological oxidation of NO_2 to NO_3 in the reach at 20 °C	[0.2,1.19]	0.430	3
SOL_CBN.sol (r)	Organic carbon content in soil	[−0.75,0.08]	−0.448	4
RS4.swq (v)	Rate coefficient for organic N settling in the reach at 20 °C	[0.001,0.056]	0.057	5

and then translates the demand of landuse for application by the spatial allocation module (Verburg, 2010). Thus, the demand module answers, "at what rate does landuse change during a certain time?" While the spatial allocation module addresses the issue, "what are the probable classes of landuse change in each grid during the specified period?"

The SRB model was calibrated using the landuse map of 2009 to simulate that of 2014 (Fig. 3). The simulated map of 2014 was then compared with the observed landuse map of 2014. The verification error is quantified using Kappa statistical analysis (K). A value of K (0–1) closer to 1 represents better agreement between the two maps (Cohen, 1960).

$$K = \frac{Pr(a) - Pr(e)}{1 - P(e)} \quad (5)$$

Where, Pr(a) is the observed relative agreement amongst all rasters and Pr(e) is the hypothetical probability of chance of agreement.

The following Eq. (6) represents the relationship between landuse change and driving factors.

$$\log\left(\frac{P_i}{1-P_i}\right) = \beta_0 + \beta_1 X_{1,i} + \beta_2 X_{2,i} + \ldots\ldots\ldots\ldots\ldots\beta_n X_{n,i} \quad (6)$$

Where Pi is the probability of occurrence of a particular landuse type in a selected grid, X are driving factors, and β are the coefficients for each driving factors in the logistical model.

3.3. Hydrological and water quality modelling

The Soil and Water Assessment Tool (SWAT) is a physically based, continuous-time, semi-distributed model designed to analyse the surface water quality and quantity in a variety of land management practices (Arnold et al., 1998). Being non-commercial software with a user-friendly interface (ArcSWAT) and flexible data requirements, SWAT has been widely applied in hydrological analyses (Fan and Shibata, 2015; Kharel and Kirilenko, 2015; Mehdi et al., 2015).

Table 4
Performance of SWAT model in simulating daily discharge (Q) and nitrate-nitrogen loading (NO_3-N).

Criteria for model skill evaluation	Calibration		Validation	
	Q	NO_3-N	Q	NO_3-N
Nash-Sutcliffe efficiency (NSE)	0.74	0.67	0.76	0.60
Coefficient of determination (R^2)	0.80	0.68	0.81	0.79
RMSE-observation standard deviation ratio (RSR)	0.51	0.57	0.49	0.64
Percent bias in volume (PBIAS)	9.60	−10.40	1.30	38.70

In SWAT, the land phase of the hydrologic cycle is based on the water balance. The corresponding equation is as follows:

$$SW_t = SW_0 + \sum_{i=1}^{t}(R_{day} - Q_{surf} - E_a - w_{seep} - Q_{gw}) \quad (7)$$

Where, SW_t is the final soil water content (mm H_2O), SW_0 is the initial soil water content (mm H_2O), t is the time (days), R_{days} is the amount of precipitation on day i (mm H_2O), Q_{surf} is the amount of surface runoff on day i (mm H_2O), E_a is the amount of evapotranspiration on day i (mm H_2O), w_{seep} is the amount of percolation and bypass flow exiting the soil profile bottom on day i (mm H_2O), and Q_{gw} is the amount of return flow on day i (mm H_2O).

The surface runoff of the hydrological cycle is estimated using the SCS curve number procedure for which the equation is:

$$Q_{surf} = \frac{(R_{day} - I_a)^2}{(R_{day} - I_a + S)} \quad (8)$$

Where, I_a is the initial abstractions, including surface storage, interception and infiltration prior to runoff (mm H_2O), and S is the retention parameter (mm H_2O). The retention parameter varies spatially due to changes in soil, landuse management, and slope and temporary changes in the soil water content. S is defined as:

$$S = 25.4\left(\frac{1000}{CN} - 10\right) \quad (9)$$

Where CN is the curve number for the day. The CN and thus the surface runoff from the Hydrologic Response Units (HRU, basic block of SWAT) will vary as each HRU is a unique combination of soil, landuse, and slope.

SWAT is used to monitor five different pools of nitrogen in the soil as shown in Fig. 4. Two pools are inorganic forms of nitrogen (Mineral N) while the other three are organic. Nitrate falls in the former pool. For a more detailed description of SWAT simulation in the hydrology and nitrate cycle, refer to the SWAT theoretical documentation http://swat.tamu.edu.

3.3.1. Model setup

The SWAT model for the SRB has an area of 12,880 km^2. This area was sub-divided into 99 sub-basins based on drainage density. Each sub-basin was further sub-divided into Hydrologic Response Units (HRUs) which are a unique combination of landuse, soil type, and the slope within the sub-basin. In total, 989 HRUs were used in the model. The Penman-Monteith method was used to calculate the PET, while the SCS method was chosen to calculate the surface runoff.

The hydrological component of the model was calibrated and validated using the daily discharge at KH.55 station (outlet of the SRB). Daily discharge throughout the years 1990–2004 was used for calibration while that covering 2005–2014 was used for validation. Whereas,

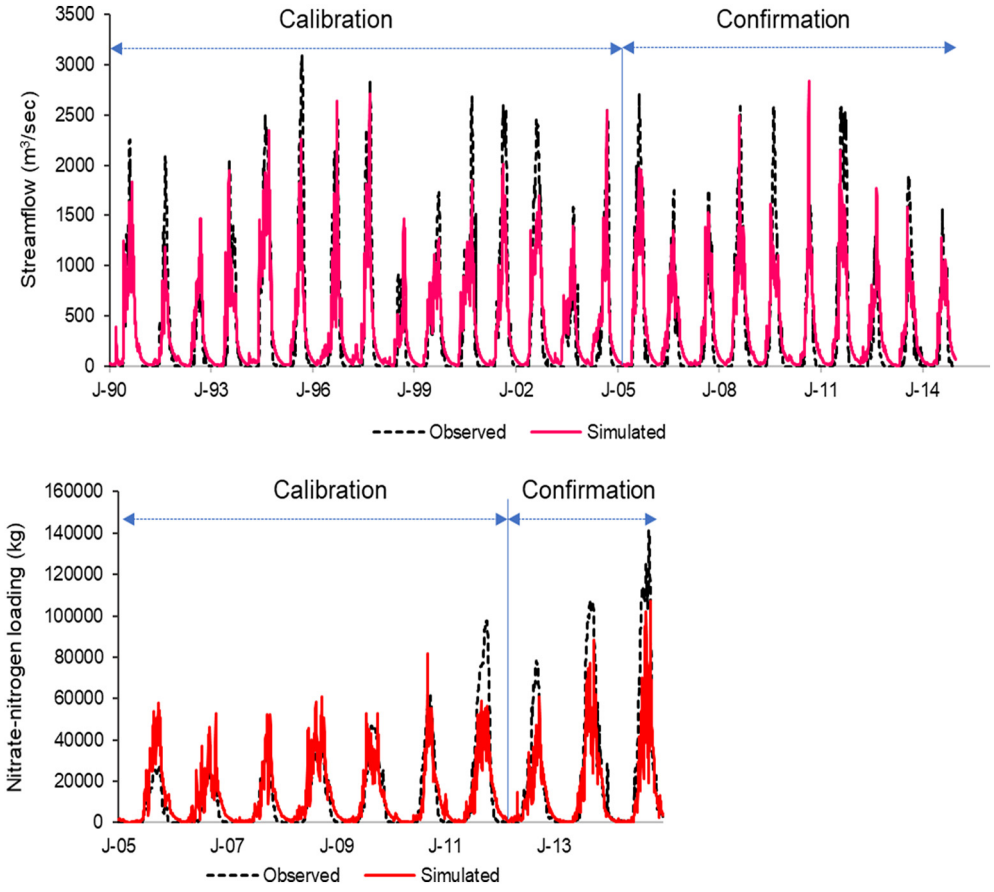

Fig. 5. Comparison between observed and simulated daily streamflow (top) and nitrate nitrogen loading (bottom) during calibration and validation (confirmation) periods at the KH 55 station

the nitrate nitrogen loading simulated by the model was calibrated using nitrate-nitrogen data at KH.55 station for seven years (2005–2011) and validated for three years (2012–2014). The model was calibrated using the automatic calibration software SWAT-CUP under SUFI-2 optimisation algorithm (Abbaspour, 2008; Arnold et al., 2012). Since flow governs water quality and in-stream processes, the model was first calibrated for discharge and then for nitrate-nitrogen load. The NSE, R^2, PBIAS, and RSR were the statistical indicators used to evaluate model performance.

Due to the sparse temporal scale of nitrate-nitrogen concentration data (two to four times a year), Load ESTimator (LOADEST) software was applied alongside the daily discharge data at KH.55 station in order to estimate the daily nitrate-nitrogen load. Load ESTimator (LOADEST) is a FORTRAN program for estimating constituent loads in streams and rivers. Given a time series of streamflow, additional data variables, and constituent concentration, LOADEST assists the user in developing a regression model for the estimation of constituent load (calibration). Explanatory variables within the regression model include various functions of streamflow, decimal time, and additional user-specified data variables (Runkel et al., 2004).

4. Results and discussion

4.1. SWAT model calibration and validation

The SWAT model was calibrated and validated for daily streamflow and nitrate-nitrogen loading only at the basin outlet (Kh.55 station). The key parameters influencing the hydrological processes and nitrogen cycle were selected for calibration from previous studies (El-Khoury et al., 2015; Oeurng et al., 2016; Trang et al., 2017). The five sensitive parameters for streamflow and nitrate-nitrogen loading with detailed descriptions are listed in Table 3. The agreement between observed and simulated flow was measured using NSE, R^2, PBIAS, and RSR for both calibration (1990–2004) and validation (2005–2014) periods and a five-year warming up period (1985–1989) was provided for better performance of the model (Table 4). The statistical results of model performance are: NSE = 0.74, R^2 = 0.8, PBIAS = 9.6, RSR = 0.51 and NSE = 0.76, R^2 = 0.81, PBIAS = 1.3, RSR = 0.49 during calibration and validation, respectively at Kh.55 station. Model performance in daily time step is good for the calibration and validation periods (Moriasi et al., 2007). However, the model does not predict flood peaks accurately (Fig. 5). The volume bias during the validation period is only 1.3%, implying that the calibrated SWAT model is good enough to describe the streamflow of the SRB and the optimised model parameters can be used to simulate future flow in response to climate and landuse changes. There are thirty rainfall stations near and within the basin and, therefore, the results are believed to be highly reliable for replicating future changes, since the model was validated with observed streamflow.

The most sensitive parameters for nitrate-nitrogen loading together with their ranges and final values are listed in Table 3. To confirm the model performance, the simulated nitrate-nitrogen loading was compared with that of the observed. The Load ESTimator (LOADEST) model was used to develop daily time series nitrate-nitrogen loading at the outlet station. The model performance statistics are listed in Table 4. The NSE, R^2, PBIAS, and RSR values during the calibration period (2005–2011) are 0.67, 0.68, −10.4, and 0.57, respectively. The model was validated over three years (2012–2014) and the NSE, R^2, PBIAS, and RSR were 0.6, 0.79, 38.7, 0.48, respectively. Volume bias (Fig. 5) during the validation period is much higher compared to the calibration

Table 5
Performance of linear bias correction method (results are shown only for ACCESS-CSIRO-CCAM Regional Climate Model).

Station ID	Elevation (m)	SD (mm)	R^2	RMSE (mm)
Rainfall				
356011	318.14			
Raw		5.20	0.31	6.00
Bias corrected		3.79	0.39	3.12
356014	196.40			
Raw		6.53	0.42	4.93
Bias corrected		1.89	0.78	3.79
352006	178.10			
Raw		5.86	0.44	6.76
Bias corrected		4.90	0.49	4.52
352010	163.81			
Raw		6.26	0.48	4.91
Bias corrected		3.81	0.73	3.72
356003	153.47			
Raw		7.94	0.41	4.92
Bias corrected		5.25	0.53	3.21
Maximum temperature				
356301	194.95			
Raw		5.46	0.80	4.55
Bias corrected		4.7	0.82	2.05
357301	147.63			
Raw		5.58	0.73	4.86
Bias corrected		3.93	0.76	2.93
Minimum temperature				
356301	194.95			
Raw		4.71	0.86	3.83
Bias corrected		2.73	0.91	2.05
357301	147.63			
Raw		5.59	0.89	3.47
Bias corrected		3.46	0.93	1.07

period but many studies suggest that for water quality simulation this result is sufficient for daily time steps. However, from the NSE and R^2 perspective, model performance is good for simulating daily load. As nitrate is a highly transient chemical, low values for NO_3-N can be expected during simulation (El-Khoury et al., 2015). Overall, the model can be used with a reasonably high degree of confidence to simulate future flow and nitrate-nitrogen loading.

4.2. Future climate change projection

Future climate was represented by temperature (T_{max}, T_{min}) and precipitation using three RCMs (ACCESS-CSIRO-CCAM, CNRM-CM5-CSIRO-CCAM, and MPI-ESM-LR-CSIRO-CCAM) and two emission scenarios: RCP 4.5 (medium) and RCP 8.5 (high). The bias corrected data was compared with the baseline (1975–2009) climate data to calculate the absolute change in temperature and precipitation. Before constructing future climate scenarios, performance of linear bias correction was analysed. The performance was evaluated comparing raw data of RCM with bias corrected RCM data using statistical indicators such as R^2, standard deviation (SD) and Root Mean Square Error (RMSE). The results show the improvement in R^2 and minimization of SD and RMSE after bias correction (Table 5). The Table 5 depicts the performance for only ACCESS-CSIRO-CCAM Regional Climate Model and the performance is also similar with other two RCMs.

The baseline average annual rainfall, T_{max}, and T_{min} around the outlet station are 1608 mm, 31.5, and 21 °C, respectively. All RCMs agreed that maximum and minimum temperatures during the future periods are projected to increase. The absolute ensemble changes in average annual minimum temperature are 1.5, 2.1, and 2.6 °C under RCP 4.5 and 1.7, 2.7, and 4.7 °C under RCP 8.5 during the 2020s, 2050s, and 2080s, respectively. Similarly, the ensemble changes in average annual maximum temperature are 1.6, 1.5, and 1.7 °C under RCP 4.5 and 1.2, 2.3, and 4.0 °C under RCP 8.5 during the 2020s, 2050s, and 2080s, respectively. The increasing rate of minimum temperature was found to be considerably higher than that of the maximum temperature. Compared to the summer season, the increasing rate of both minimum and maximum temperatures was higher during the rainy and winter seasons for both RCP scenarios. Similar results are reported in the South-east Asian countries (Aung et al., 2016; Trang et al., 2017). In summary, temperatures during the future periods are projected to rise for all seasons, with the rate increase being higher under RCP 8.5 than RCP 4.5, in later years. Fig. 6 (top and middle) shows the absolute change in temperature with respect to the baseline period.

The ACCESS RCM shows that rainfall during the future periods for both RCP scenarios is expected to increase, whereas the other two RCMs show a decrease in rainfall for the entire time series under both scenarios. The ensemble of three RCMs shows a decrease in average annual rainfall of 3.7, 2.3, and 4% during the 2020s, 2050s, and 2080s under the RCP 4.5 scenario. However, under the RCP 8.5 scenario, rainfall will decrease by 5, 3.9, and 7.2% during the 2020s, 2050s, and 2080s, respectively. The decreasing rate was found to be low during the 2050s for both scenarios. Average rainfall during winter is expected to increase by a certain amount, whereas the results show a significant decrease during the summer and rainy seasons for both climate scenarios. The predicted future change in rainfall with respect to the baseline value is represented by Fig. 6 (bottom).

4.3. Future landuse change projection

4.3.1. Economic scenario

The scenario focusing on the economic growth of the region shows that more than half of the basin area is expected to be covered by rubber plantation if the rate of increase remains the same as in the past. In this scenario, a distinct positive change can be seen on urban, rubber farm, and miscellaneous landuse types but crops, paddy, and forest will decrease by a high percentage. By the year 2100 the forest area is expected to decrease by 100%, meanwhile, rubber farms would increase by 275%. Fig. 7 shows the future landuse of the basin during the years 2030, 2050, and 2080.

4.3.2. Conservation scenario

Under the conservation scenario (increase in forest by 25% of total land area by 2100), natural forest will gradually start to expand from the natural park and cover just over 20% of the area by the middle of the century. This scenario restricts the rapid expansion of built-up area, covering just over 8% of the total landuse area by 2100. The basin will also experience a decrease in rubber farms and paddy fields to compensate for the expanding forest. In this scenario, the forest, crop, and built-up area (urban) will change incrementally with respect to the baseline landuse map. An incremental change in forest of just over 58% can be seen by 2100. The crop area will experience a constant positive change throughout the time by 67% (Fig. 7). Since no change in water bodies is allowed, by the end of this century they will cover the same water area as the baseline. Relative changes for both landuse scenarios with respect to the baseline (2009) map are summarised in Table 6.

4.4. Climate change and landuse change impacts on streamflow

Climate change impacts on streamflow were estimated by keeping the landuse constant with the baseline (2009). The simulated flow under different climate change (RCP 4.5 and RCP 8.5) scenarios for three different time windows was compared with the baseline (1990–2009) flow 350 m^3/s to calculate future changes in streamflow. The annual precipitation of the basin is expected to decrease during the future periods under both climate scenarios, and a strong correlation (0.89) was found between precipitation and streamflow changes. The predicted decrease in rainfall had a dramatic impact on future streamflow. The basin streamflow showed a greater impact from climate change than landuse change. Although the flow in different

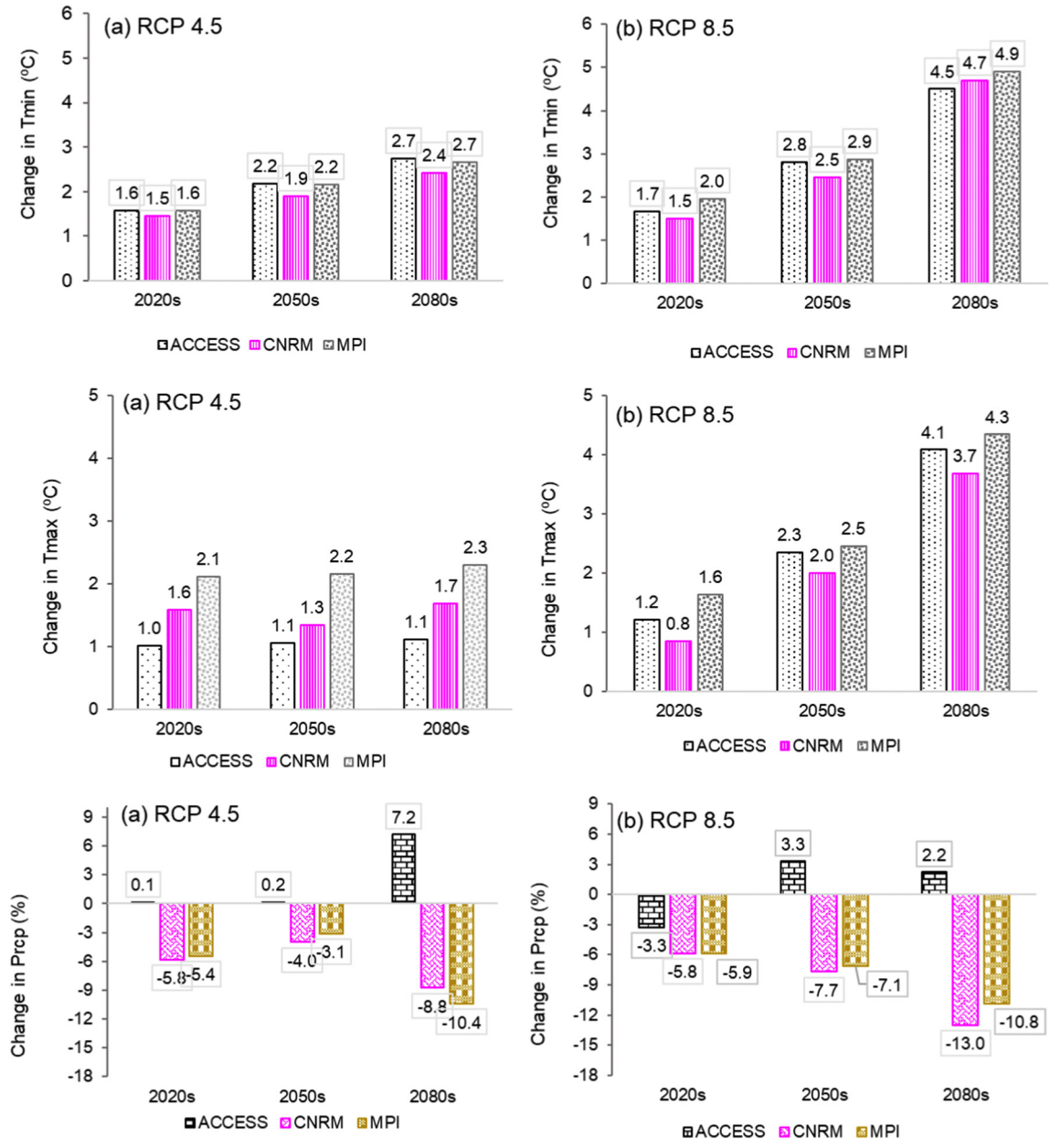

Fig. 6. Absolute change with respect to the baseline period (1975–2009) in minimum temperature (top), maximum temperature (middle), and relative change in precipitation (bottom).

scenarios is analysed by splitting the time into three time windows, the annual flow was estimated to decrease during the future periods. The annual changes in average streamflow due to climate change only is expected to decrease by 20, 14.4, and 24.1% under RCP 4.5 scenario and 22, 18.7, and 30.9% under RCP 8.5 during the 2020s, 2050s, and 2080s periods, respectively (Fig. 8). The basin is experiencing high seasonal variability in precipitation and flow volume. Since more than 90% of annual precipitation and flow occurs in the rainy season, the other two seasons are less influential on annual flow volume. In particular, winter flow is expected to increase by 5.1, 18.8, and 16.8% under RCP 4.5 and 1.5, 14.4, and 8.1% under RCP 8.5 for the 2020s, 2050s, and 2080s, respectively. Meanwhile, streamflow during the summer and rainy seasons is expected to decrease for both climate scenarios. Other studies in Asian basins (Kim et al., 2013; Park et al., 2011; Trang et al., 2017) also report big impacts from climate change on streamflow because of future changes in precipitation. The predicted flow of the basin is expected to decrease for all the decades under both RCPs scenarios, with the rate decreasing less during the 2040s, 2050s, and 2060s compared to other decades.

In addition, the individual as well as combined impacts of climate and landuse change on streamflow were evaluated by considering two landuse change scenarios. The flow reduction rate is demoted under both landuse change scenarios, implying it has a positive impact on flow but the effect is tiny compared to that of climate change. Simulated landuse maps for the years 2030, 2050, and 2080 were used to estimate the potential impacts of landuse change on the outlet flow of the SRB. The combined impact under economic landuse change on average annual streamflow is expected to decrease by 16.9, 10.1, and 18.9% under RCP 4.5 and 16.9, 12.5, and 23.4% under RCP 8.5 during the 2020s, 2050s, and 2080s, respectively. Similarly, the combined effects under the conservation landuse change scenario are expected to decrease the streamflow by 13.8, 9.8, and 18.2% under RCP 4.5 and 13.5, 12.8, and 25.1% under RCP 8.5 during the 2020s, 2050s, and 2080s, respectively. The decrease in streamflow can be attributed to increase in

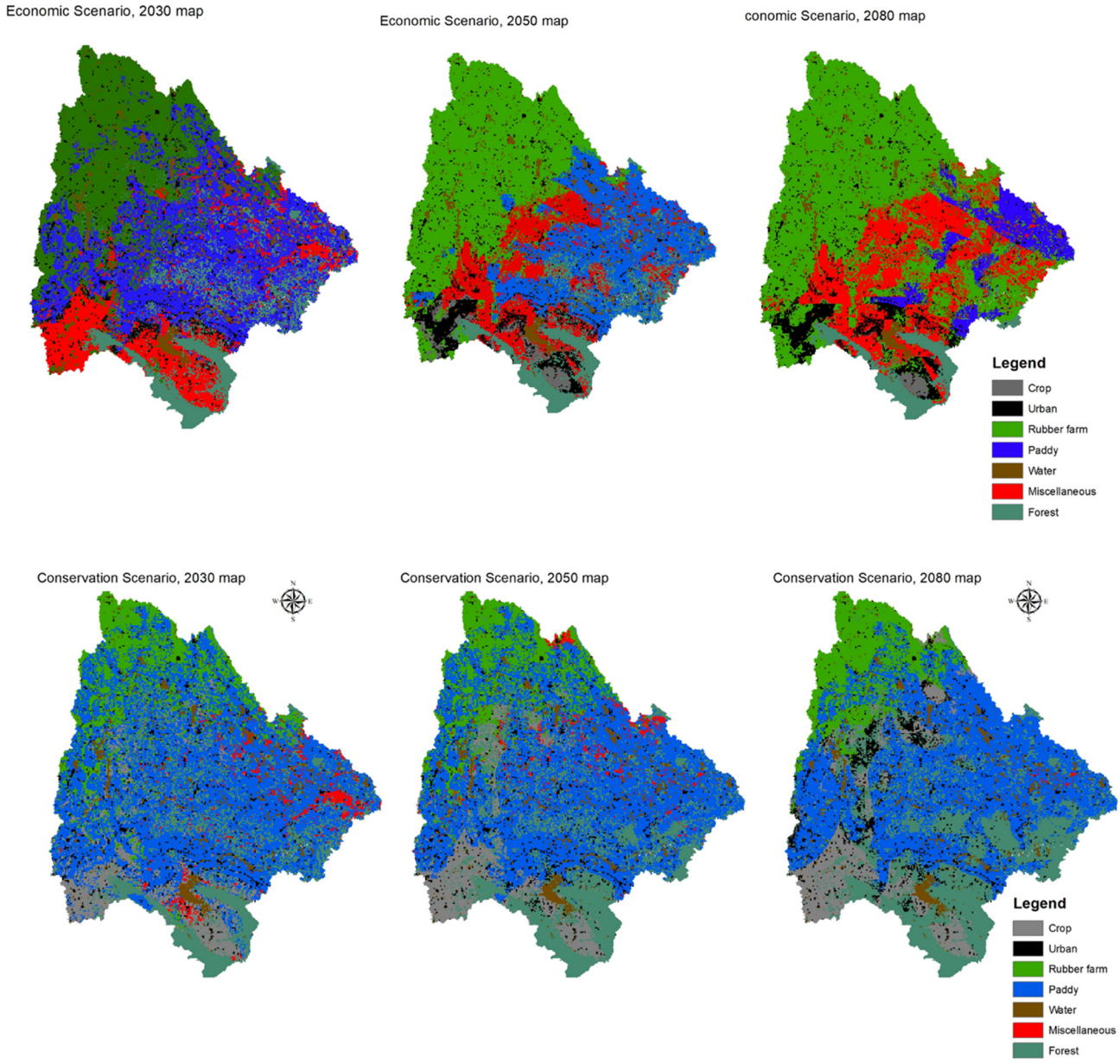

Fig. 7. Projected landuse map for economic (top) and conservation (bottom) scenarios.

evapotranspiration as a result of increase in temperature and decrease in rainfall in future. Table 7 shows the changes in future flow under the individual and combined impact of climate and landuse change. Finally, basin streamflow is more sensitive to climate change than landuse change. Nevertheless, climate and landuse change are concurrent phenomenon and, therefore, the landuse change impact should not be overlooked. However, landuse change has significantly less impact on annual flow for both landuse change scenarios.

Table 6
Projected landuse area (km^2) in the SRB during the years 2030, 2050, and 2080, and relative changes (%) with respect to the baseline area of 2009. The number in italics in parenthesis is percentage change.

Landuse type (km^2)	2030		2050		2080	
	Economic	Conservation	Economic	Conservation	Economic	Conservation
Crop (764.2)	0 *(−100)*	1155.43 *(51)*	337.5 *(−55)*	1150.2 *(50)*	125.2 *(−84)*	1281.43 *(67)*
Urban (492.4)	642.24 *(30)*	483.5 *(−2)*	994.12 *(102)*	546.4 *(11)*	1081.81 *(120)*	853.12 *(74)*
Planted trees (1876.27)	3954.9 *(110)*	1768.7 *(−6)*	4814.37 *(156)*	1571.84 *(−16)*	6807.25 *(262)*	1601.75 *(−15)*
Paddy (6165.38)	4139.68 *(−33)*	6205.3 *(1)*	2757.56 *(−55)*	5831.6 *(−5)*	966.5 *(−84)*	4987.2 *(−20)*
Water (639.74)	633.87 *(−1)*	633.87 *(−1)*	633.87 *(−1)*	633.87 *(−1)*	633.87 *(−1)*	633.87 *(−1)*
Miscellaneous (747)	1655.2 *(122)*	362.75 *(−51)*	1840.06 *(146)*	274.25 *(−64)*	2556.37 *(242)*	13.12 *(−98)*
Forest (2192.3)	1797.06 *(−18)*	2213.4 *(1)*	1445.5 *(−34)*	2814.75 *(28)*	652 *(−70)*	3452.5 *(58)*

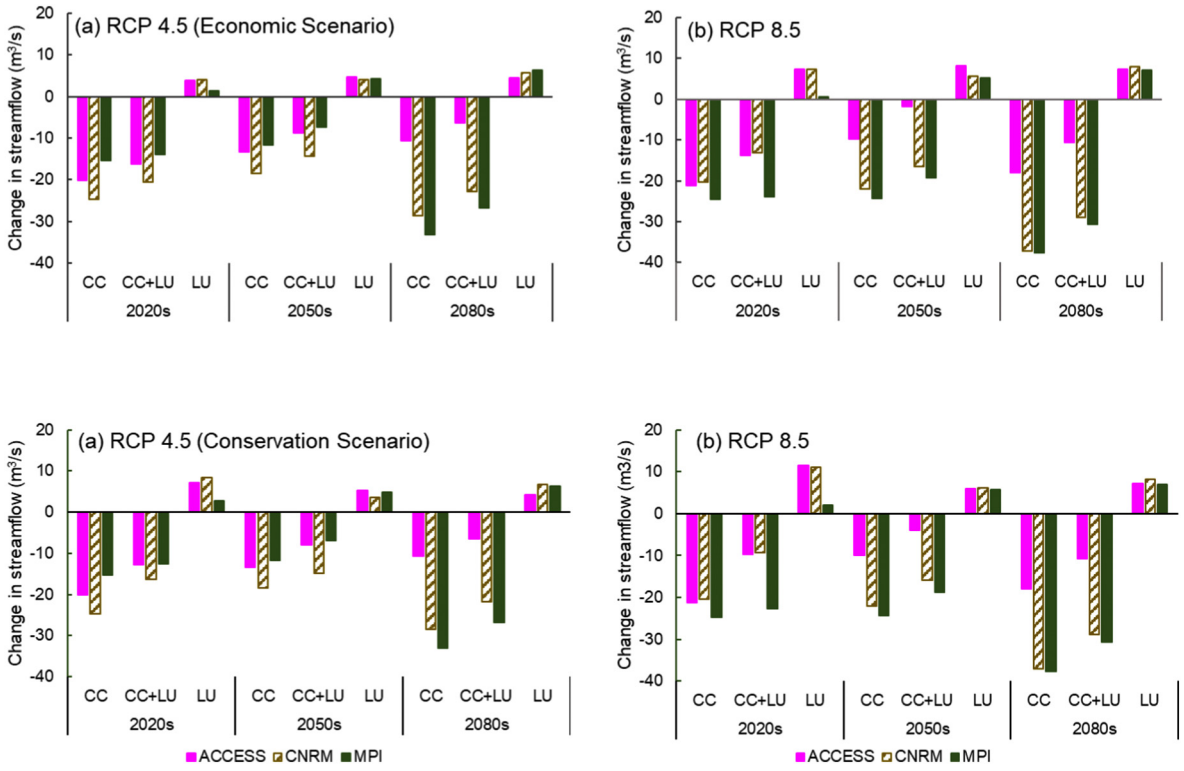

Fig. 8. Individual and combined impacts of climate and landuse change on streamflow under economic (top) and conservation (bottom) scenarios.

4.5. Climate and landuse change impacts on nitrate-nitrogen loading

LOADEST model was used to develop daily time series data for nitrate-nitrogen loading at the outlet station of the SRB and water quality model calibration and validation. The SWAT model was used to simulate NO_3-N under the two climate scenarios RCP 4.5 and 8.5 for three time windows (the 2020s, 2050s, and 2080s), by keeping the landuse constant. During the historical period (1995–2009) the estimated nitrate nitrogen loading shows an increasing trend. High seasonal variability in loading can be seen, with the rainy season accounting for more than 85% of annual nitrate nitrogen load whereas only 3.8% of the annual load was observed during summer. During the historical period, agricultural land was dominant, so an increasing trend was observed in nitrate nitrogen load. Loading is the function of streamflow, rainfall, topography, landuse type, etc. with flow playing a vital role in generating loading, and a correlation was found between flow and nitrate-nitrogen loading of 0.86. Loading magnitude varies with landuse type at sub-basin level, but research focuses only on the basin scale and the estimated nitrate load at the SRB outlet was 333.2 kg/km^2, despite the agricultural sub-basin having a higher yield than others.

The SRB annual average nitrate nitrogen loading is projected to decrease by 11.1, 1.3, and 10.1% under RCP 4.5 and 15, 5, and 15% under RCP 8.5 during the 2020s, 2050s, and 2080s, respectively compared to the baseline period (1995–2009). Fig. 9 shows a comparison between future and historical nitrate nitrogen loading under both climate change scenarios. Nitrate nitrogen loading is the function of streamflow and with flow being highly seasonal, the same results were reflected for nitrate yield as well. Due to climate change only, nitrate nitrogen loading

Table 7
Projected ensemble change (%) of average annual streamflow under individual and combined climate and landuse change scenarios.

	Only climate change (CC)		Combined climate and landuse change (CC + LU)				Only landuse change (LU)			
			Economic scenario		Conservation scenario		Economic scenario		Conservation scenario	
	RCP 4.5	RCP 8.5	RCP 4.5	RCP 8.5	RCP 4.5	RCP 8.5	RCP 4.5	RCP 8.5	RCP 4.5	RCP 8.5
2020s										
Annual	−20	−21.8	−13.3	−16.7	+6.5	−13.6	6.7	5.1	26.5	8.2
Summer	−20.8	−16.5	+0.56	+3.05	+33.3	+3	21.3	19.5	54.1	19.5
Rainy	−21.9	−23.8	−13.6	−17.2	+6.1	−13.3	8.3	6.6	28	10.5
Winter	+6	−1.2	−18.5	−22.8	0.4	−27.4	−24.5	−21.6	−5.6	−26.2
2050s										
Annual	−14	−18.7	−9.9	−12.1	−9.8	−10.6	4.1	6.6	4.2	8.1
Summer	−15	−23	+2.2	−6.5	2.4	−6.5	17.2	16.5	17.4	16.5
Rainy	−17	−21	−10.2	−12.2	−9.5	−10	6.8	8.8	7.5	11
Winter	+20	+21.5	−13.5	−16.1	−17.6	−20.5	−33.5	−37.6	−37.6	−42.0
2080s										
Annual	−24	−30.6	−15.8	−23.2	−16.2	−23.2	8.2	7.4	7.8	7.4
Summer	−21	−21.7	−7.9	−8.4	−7.1	−8.1	13.1	13.3	13.9	13.6
Rainy	−27.5	−34.5	−16.4	−24.3	−16.5	−24	11.1	10.2	11	10.5
Winter	+17	+9	−13.9	−17.8	−18.4	−22.3	−30.9	−26.8	−35.4	−31.3

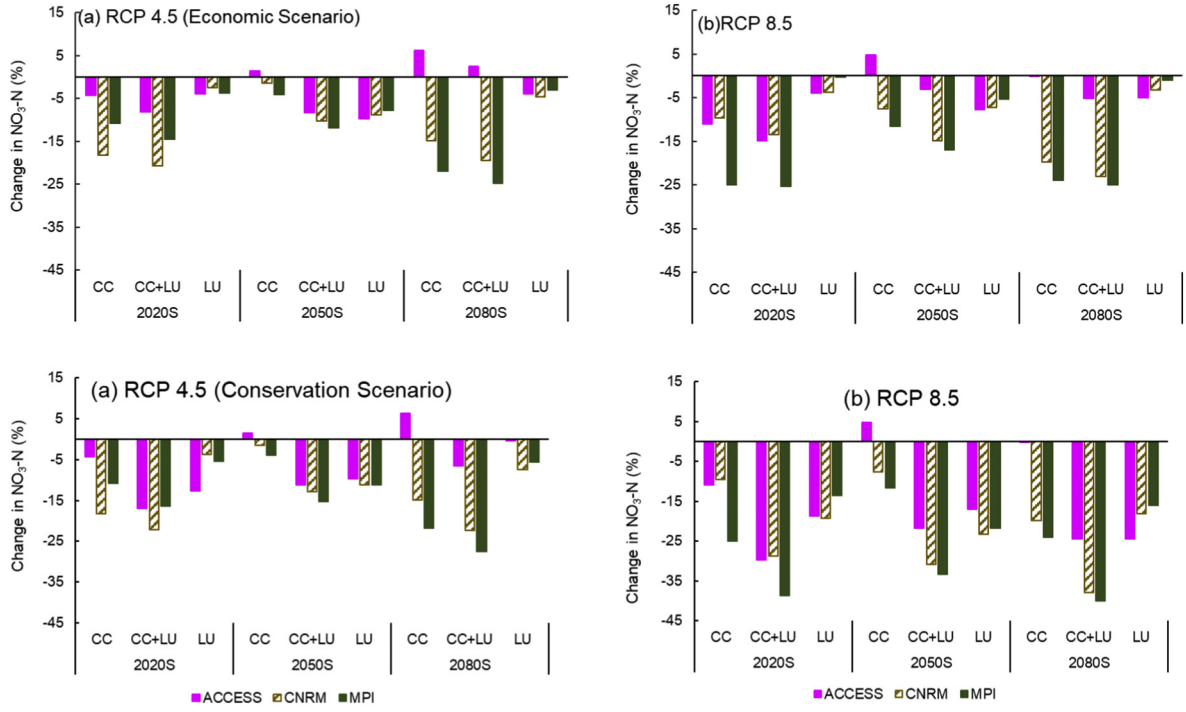

Fig. 9. Individual and combined impacts of climate and landuse change on nitrate-nitrogen loading under economic (top) and conservation (bottom) scenarios.

decreased in the summer and rainy seasons and increased in winter for both RCP scenarios.

The ACCESS RCM projected the increase the nitrate nitrogen loading in future but the other two RCMs did not agree with the ACCESS model and were predicted to decrease for all coming decades as compared with the baseline period under RCP 4.5 and RCP 8.5. Decadal change in nitrate nitrogen loading and the ensemble of three RCMs show that nitrate nitrogen loading is expected to decrease during all decades, but this is greater in later decades.

Under the economic scenario, rubber farms and paddy are the dominant landuse classes, and crops, paddy, and forest are dramatically decreasing. The decreasing rate of average annual nitrate nitrogen loading under the combined scenarios is 14, 10, and 14% under RCP 4.5 and 18, 12, and 18% under RCP 8.5 during the 2020s, 2050s, and 2080s, respectively. Simulated maps for the years 2030, 2050, and 2080 were used to develop the future SWAT model for the 2020s, 2050s, and 2080s. The results show that nitrate nitrogen loading decreased for all seasons with greater decreases in the summer season. The rainy season accounted for more than 85% of annual load and the rate of decrease is low compared to the other two seasons. Table 6 shows the annual and seasonal changes in nitrate nitrogen loading under individual and combined scenarios, with the relative changes calculated on the basis of an ensemble of three RCM outputs.

Likewise, under the conservation scenario, landuse change forced a decrease in the nitrate nitrogen loading during all three seasons. The conservation scenario was developed to increase the forest to 25% of total landuse by the end of 2100. Landuse change enhances the reduction by 5 to 10% of annual loading. The nitrate-nitrogen loading is sensitive to both climate and landuse change. The relative decrease in nitrate nitrogen loading under the conservation scenario is 18.13, 13.03, and 18.8% under RCP 4.5 and 18.9, 14.4, and 21.01% under RCP 8.5 during the 2020s, 2050s, and 2080s, respectively (Table 8).

5. Conclusions

This study quantifies the individual and combined impacts of climate and landuse change on streamflow and nitrate loading in the SRB. Future landuse maps were simulated using the Dyna-CLUE model and future climate data extracted from CMIP5 Regional Circulation Models (RCMs) under two climate scenarios RCP 4.5 and RCP 8.5 for

Table 8
Projected ensemble change (%) in nitrate-nitrogen loading under climate and landuse change scenarios.

	Only climate change (CC)		Combined climate and land use change (CC + LU)				Only land use change (LU)			
			Economic scenario		Conservation scenario		Economic scenario		Conservation scenario	
	RCP 4.5	RCP 8.5	RCP 4.5	RCP 8.5	RCP 4.5	RCP 8.5	RCP 4.5	RCP 8.5	RCP 4.5	RCP 8.5
Annual	−11.1	−15.0	−14.0	−18.0	−18.1	−18.9	−2.9	−3.0	−7.0	−3.9
Summer	−33.4	−32.0	−41.2	−41.2	−22.6	−22.5	−7.8	−9.2	10.8	9.5
Rainy	−13.2	−17.2	−14.6	−17.2	−19.2	−18.5	−1.4	0.0	−6.0	−1.3
Winter	−9.6	−15.6	−30.0	−34.7	−34.7	−40.2	−20.4	−19.1	−25.1	−24.6
Annual	−1.3	−5.0	−10.0	−12.0	−13.0	−14.4	−8.7	−7.0	−11.7	−9.4
Summer	−23.2	−30.6	−40.3	−45.8	−36.1	−35.1	−17.1	−15.2	−12.9	−4.5
Rainy	−4.8	−8.2	−9.8	−11.4	−12.5	−14.2	−5.0	−3.2	−7.7	−6.0
Winter	7.2	6.0	−1.8	−22.4	−29.8	−29.3	−9.0	−28.4	−37.0	−35.3
Annual	−10.1	−15.0	−14.0	−18.0	−18.8	−21.0	−3.9	−3.0	−8.7	−6.0
Summer	−28.1	−32.9	−51.8	−57.9	−35.5	−43.7	−23.7	−25.0	−7.4	−10.8
Rainy	−14.6	−18.7	−15.0	−17.6	−19.4	−21.2	−0.4	1.1	−4.8	−2.5
Winter	7.0	1.2	−20.6	−24.8	−28.1	−30.8	−27.6	−26.0	−35.1	−32.0

three different time horizons 2020s, 2050s, and 2080s. Two landuse change scenarios "Economic" and "Conservation" were developed for future periods. The economic scenario follows past trends, while the conservation scenario allows proliferation of the forest area (25% of the total basin area by 2100). Under the economic scenario, more than 50% of the basin is expected to be covered by rubber farms. Thus, this scenario depletes a substantial area under paddy, crops, and forest. Under the conservation scenario, the forest area is protected and proliferated, thus controlling land availability for rubber farms and paddy fields. For both landuse change scenarios, maps for the years 2030, 2050, and 2080 were used in SWAT for future analysis. The pre-existing bias in the climate data was corrected by linear scaling method before being fed into the hydrological model. SWAT model was used to simulate future streamflow and nitrate loading at the outlet of the SRB. The impacts were analysed in three cases — climate change alone, land use change alone, and the combined effect of both climate change and landuse change.

Climate analysis showed an increase in the future temperatures of the basin and a decrease in rainfall compared to the baseline period for all time horizons and under both climate scenarios. Hydrological analysis depicts that the winter and rainy season flows of the SRB will be lower for all time horizons. However, winter flow was observed to receive some increase when the model was subjected to climate change only. Similar results were expected for nitrate nitrogen loading in the river as well. The landuse change alone scenario had a positive impact on streamflow whereas nitrate nitrogen loading was seen to decrease under both landuse change scenarios. Comparatively, the climate change alone scenario showed a significant impact on streamflow. However, the impacts were seen to be equal to nitrate nitrogen loading. Finally, combined landuse and climate change forcing decreased both streamflow and nitrate nitrogen loading in the SRB. Based on the results and their variability in terms of forcing (climate and land use), it can be concluded that planning and management of the individual and combined impacts of climate and landuse change are crucial for the sustainable management of water resources in SRB.

Acknowledgements

The authors would like to acknowledge sincere thanks to Royal Irrigation Department (RID), Pollution Control Department (PCD) and Thai Meteorological Department (TMD), of Thailand for providing required data for this research.

References

Abbaspour, 2008. SWAT calibrating and uncertainty programs. A User Manual. Eawag Zurich, Switzerland.
Arnold, J.G., Srinivasan, R., Muttiah, R.S., Williams, J.R., 1998. Large area hydrologic modeling and assessment part I. Model Development 1. Wiley Online Library.
Arnold, J.G., Moriasi, D.N., Gassman, P.W., Abbaspour, K.C., White, M.J., Srinivasan, R., Van Liew, M.W., 2012. SWAT: model use, calibration, and validation. Trans. ASABE 55 (4), 1491–1508.
Aung, M., Shrestha, S., Weesakul, S., Shrestha, P., 2016. Multi-model climate change projections for Belu River Basin, Myanmar under Representative Concentration Pathways. Journal of Earth Science & Climatic Change 7 (1), 1–13.
Berka, C., Schreier, H., Hall, K., 2001. Linking water quality with agricultural intensification in a rural watershed. Water Air Soil Pollut. 127 (1), 389–401.
Blake, D.J., Pitakthepsombut, R., 2006. Situation Analysis.
Cohen, J., 1960. A coefficient of agreement for nominal scales. Educ. Psychol. Meas. 20 (1), 37–46.
Cuo, Y., Zhang, Y., Gao, Z., Hao, L. Cairang, 2013. The impacts of climate change and land cover/use transition on the hydrology in the upper Yellow River basin, China. J. Hydrol. 502 (2013):37–52. https://doi.org/10.1016/j.jhydrol.2013.08.003.
Daniel, T., Sharpley, A., Lemunyon, J., 1998. Agricultural phosphorus and eutrophication: a symposium overview. J. Environ. Qual. 27 (2), 251–257.
El-Khoury, A., Seidou, O., Lapen, D., Que, Z., Mohammadian, M., Sunohara, M., Bahram, D., 2015. Combined impacts of future climate and land use changes on discharge, nitrogen and phosphorus loads for a Canadian river basin. J. Environ. Manag. 151, 76–86.
Fan, M., Shibata, H., 2015. Simulation of watershed hydrology and stream water quality under land use and climate change scenarios in Teshio River watershed, northern Japan. Ecol. Indic. 50, 79–89.
Heathwaite, A.L., 2010. Multiple stressors on water availability at global to catchment scales: understanding human impact on nutrient cycles to protect water quality and water availability in the long term. Freshw. Biol. 55 (2010), 241–257.
Hunter, P., 2003. Climate change and waterborne and vector-borne diseases. J. Appl. Microbiol. 94, 37S–46S.
Ines, A.V., Hansen, J.W., 2006. Bias correction of daily GCM rainfall for crop simulation studies. Agric. For. Meteorol. 138 (1), 44–53.
IPCC, 2014. Climate change 2014: synthesis report. In: Core Writing Team, Pachauri, R.K., Meyer, L.A. (Eds.), Contribution of Working Groups I, II and III to the Fifth Assessment Report of the Intergovernmental Panel on Climate Change. IPCC, Geneva, Switzerland (151 pp).
Kharel, G., Kirilenko, A., 2015. Considering climate change in the estimation of long-term flood risks of Devils Lake in North Dakota. J. Am. Water Resour. Assoc. 51 (5), 1221–1234.
Kim, Choi, J., Choi, C., Park, S., 2013. Impacts of changes in climate and land use/land cover under IPCC RCP scenarios on streamflow in the Hoeya River Basin, Korea. Sci. Total Environ. 452, 181–195.
Li, B.F., Chen, Y.N., Chen, Z.S., et al., 2012. The effect of climate change during snowmelt period on streamflow in the mountainous areas of Northwest China. Acta Geograph. Sin. 67 (11), 1461–1470 2012.
Li, C., Sinha, E., Horton, D.E., Diffenbaugh, N.S., Michalak, A.M., 2014. Joint bias correction of temperature and precipitation in climate model simulations. J. Geophys. Res. Atmos. 119 (23).
Mehdi, B., Ludwig, R., Lehner, B., 2015. Evaluating the impacts of climate change and crop land use change on streamflow, nitrates and phosphorus: a modeling study in Bavaria. J. Hydrol. 4, 60–90.
Moriasi, D.N., Arnold, J.G., Van Liew, M.W., Bingner, R.L., Harmel, R.D., Veith, T.L., 2007. Model evaluation guidelines for systematic quantification of accuracy in watershed simulations. Trans. ASABE 50 (3), 885–900.
Murray-Hudson, M., et al., 2006. Scenarios of the impact of local and upstream changes in climate and water use on hydro- ecology in the Okavango Delta, Botswana. J. Hydrol. 331, 73–84.
Neitsch, S.L., Arnold, J.G., Kiniry, J.R., Williams, J.R, 2011. Soil and Water Assessment Tool Theoretical Documentation Version 2009. Texas Water Resources Institute.
Novotny, E.V., Stefan, H.G., 2007. Stream flow in Minnesota: Indicator of climate change. J. Hydrol. 334:319–333. https://doi.org/10.1016/j.jhydrol.2006.10.011.
Oeurng, C., Cochrane, T.A., Arias, M.E., Shrestha, B., Piman, T., 2016. Assessment of changes in riverine nitrate in the Sesan, Srepok and Sekong tributaries of the Lower Mekong River Basin. J. Hydrol. 8, 95–111.
Park, M.-J., Joh, H.-K., Shin, H.-J., Kwon, H.-J., Srinivasan, R., Kim, S.-J., 2011. Assessment of MIROC3. 2 HiRes climate and CLUE-s land use change impacts on watershed hydrology using SWAT. Trans. ASABE 54 (5), 1713–1724.
Pulido-Velazquez, M., Peña-Haro, S., García-Prats, A., Mocholi-Almudever, A., Henriquez-Dole, L., Macian-Sorribes, H., Lopez-Nicolas, A., 2015. Integrated assessment of the impact of climate and land use changes on groundwater quantity and quality in the Mancha Oriental system (Spain). Hydrol. Earth Syst. Sci. 19 (4), 1677–1693.
Runkel, R.L., Crawford, C.G., Cohn, T.A., 2004. Load estimator (LOADEST): a FORTRAN program for estimating constituent loads in streams and rivers. U.S. Geological Survey Techniques and Methods Book 4, Chapter A5.
Shrestha, S., Muangthong, S., 2014. Assessment of surface water quality of Songkhram River (Thailand) using environmetric techniques. International Journal of River Basin Management 12 (4), 341–356.
Shrestha, S., Shrestha, M., Babel, M.S., 2016. Modelling the potential impacts of climate change on hydrology and water resources in the Indrawati River Basin, Nepal. Environ. Earth Sci. 75 (4), 1–13.
Shrestha, M., Acharya, S.C., Shrestha, P.K., 2017. Bias correction of climate models for hydrological modelling–are simple methods still useful? Meteorol. Appl. 24 (3), 531–539.
Teutschbein, C., Seibert, J., 2012. Bias correction of regional climate model simulations for hydrological climate-change impact studies: review and evaluation of different methods. J. Hydrol. 456, 12–29.
Trang, N.T.T., Shrestha, S., Shrestha, M., Datta, A., Kawasaki, A., 2017. Evaluating the impacts of climate and land-use change on the hydrology and nutrient yield in a transboundary river basin: a case study in the 3S River Basin (Sekong, Sesan, and Srepok). Sci. Total Environ. 576, 586–598.
Tu, J., 2009. Combined impact of climate and land use changes on streamflow and water quality in eastern Massachusetts, USA. J. Hydrol. 379 (3), 268–283.
Van Vuuren, D.P., Edmonds, J., Kainuma, M., Riahi, K., Thomson, A., Hibbard, K., ... Lamarque, J.-F., 2011. The representative concentration pathways: an overview. Clim. Chang. 109 (1–2), 5.
Verburg, 2010. The CLUE model. Hands-on Exercises. Course Material. vol. 53. Institute for Environmental Studies, University of Amsterdam.
Verburg, & Overmars, 2009. Combining top-down and bottom-up dynamics in land use modeling: exploring the future of abandoned farmlands in Europe with the Dyna-CLUE model. Landsc. Ecol. 24 (9), 1167.
Zhang, Nan, Z., Xu, Y., Li, S., 2016. Hydrological impacts of land use change and climate variability in the headwater region of the Heihe River Basin, Northwest China. PLoS One 11 (6), e0158394.